

Age Constraints of Udayagiri Domain of Nellore Schist Belt by Xenotime Dating around Pamuru, Prakasam District, Andhra Pradesh

SANKHA DAS¹, DEVASHEESH SHUKLA¹, SANTANU BHATTACHARJEE² and SUMIT KUMAR MITRA¹

¹Geological Survey of India, SU: AP, SR, Project STM, Hyderabad - 500 068

²EPMA Laboratory, Petrology Division, GSI, SR, Hyderabad - 500 068

Email: sankhad56@gmail.com

Abstract:- The Nellore Schist Belt (NSB) is a curvilinear Archaean schist belt, approximately 350 km long and 8-50 km wide. The Nellore Schist Belt is considered to be equivalent of the Sargur Group with a protolith age of 3.3-2.5 Ga. Stratigraphically NSB is classified as the upper western Udayagiri Domain (dominated by metasediments) and lower eastern Vinjamuru Domain (dominated by metabasalts). Metabasalts of Vinjamuru Domain have been dated as of 2654 ± 100 Ma age, but so far no dates are available for the Udayagiri Domain. During recent mapping, in the central western part of NSB, west of Pamuru town, in a metapelitic of Udayagiri Domain (consisting mainly of quartz, muscovite, paragonite, Spessartine garnet, chlorite, chloritoid and magnetite as accessory mineral) four small grains of Xenotime has been found, among which three grains have been dated. Xenotime is a rare earth phosphate mineral whose major is Yttrium orthophosphate (YPO₄). Xenotime preferentially incorporates smaller HREEs and Yttrium. Xenotime has high U content and very low initial Pb concentration, so it is ideal for U-Pb geochronology. Xenotime can be of different origin such as detrital, diagenetic, hydrothermal and metamorphic. The age calculated from xenotime with the Age Quant of SX-Peak sight software gives an average age of 1921±120 Ma. This age matches well with CHIME age of 1929±130 Ma of xenotime. All the textural and geochemical characteristics of the grains suggest that the xenotime is of retrograde metamorphic origin which occurs after D1 phase of deformation, hence constraining the upper age limit of the Udayagiri Domain to be 1929±130 Ma.

Keywords: Nellore Schist Belt, Udayagiri Domain, Xenotime, CHIME age, Andhra Pradesh.

GEOLOGICAL SETTING

The Nellore Schist Belt (NSB) is a curvilinear Archaean schist belt, extending approximately 600 km long along its N-S strike and is about 8-50 km wide. The Nellore Schist Belt is considered to be equivalent of the Sargur Group with a protolith age of 3.3-2.5 Ga (Hari Prasad et al., 1999). The NSB is thrusted over the Nallamalai Fold Belt (NFB) on its west and the Eastern Ghat Mobile Belt (EGMB) is thrusted over NSB on the eastern margin of the latter. Some recent interpretations indicate that the Kandra complex at the extreme south of NSB and Kanigiri complex at the NE part of NSB may represent dismembered ophiolite complexes (Saha et.al.2013).

Stratigraphically the NSB is divided into an (upper?) western Udayagiri Group and (lower?) eastern Vinjamuru Group (Ramam and Murty, 1997). Dobmeier and Rath (2003) have divided the NSB into an eastern Vinjamuru domain and a western Udaigiri domain. However,

subsequently (Saha et.al.2013) NSB has been divided into four tectonic units, viz. the Vinjamuru Group, the Kandra complex, the Kanigiri complex and the Udayagiri Group from older to younger. The Udayagiri Group consists mainly psammite with minor conglomerate and pelite locally intercalated with felsic volcanic rocks and relatively rare basalts and limestones which have undergone greenschist facies of metamorphism. The Vinjamuru Group is dominated by metabasalt intercalated with psammo-pelitic schist, quartzites, gneisses and migmatites and locally abundant felsic metavolcanics, marbles, calc-silicate gneisses and kyanite-sillimanite schist of amphibolite facies (Vasudevan and Rao, 1975; Narayana Rao, 1983; Ramam and Murty, 1997). However, the exact stratigraphic disposition and nature of contact between the above two groups is controversial (Ramam and Murty, 1997). On the basis of metamorphism, the contact between the Vinjamuru domain and the Udayagiri domain has been described as tectonic

(Moeen, 1998). Vasudevan et al. (1975–76, unpublished GSI report) reported a shear zone between the two domains of rocks and a possible thrust contact between them. A reported easterly dipping thrust at the contact between Vinjamuru domain and Udayagiri domain has been ruled out as the foliation here shows a steep westerly dip in rocks of both domains at the contact (Saha, 2004).

Geochronology of NSB

Metabasalt of Vinjamuru domain (from Chaganam and Chundi) of NSB is dated to be 2654 ± 100 Ma from Sm-Nd systematics, which is considered the preferred time of the formation of these volcanics, and a Sm-Nd age of 1911 ± 88 Ma obtained from the differentiated gabbros intrusive into NSB (Ravikant, 2010). Recently interpreted plagiogranite and gabbros have been dated at 1330 Ma by U-Pb dating of zircon grains from the Kandra complex (Dharma Rao et al., 2011). So far no dates are available for the metasediments of Udayagiri domain.

Present Work

In this paper an attempt has been made to constrain the age of the metasediments of Udayagiri domain of NSB, through xenotime found in a garnet–chloritoid schist of Udayagiri domain that may throw some light on the contact relationship between Udayagiri and Vinjamuru domains.

The present study area is located in central western part of the Nellore schist belt (Fig. 1), 4 km west of Pamuru town ($14^{\circ}05'46.42''N$, $79^{\circ}24'38.52''E$), in Nellore district, Andhra Pradesh. Both the Udayagiri domain and Vinjamuru domain are exposed in the study area (Fig. 1a). In the present study area Vinjamur domain mainly comprises of metabasalt/amphibolites, lit par lit injection migmatite, quartzite and intrusive granite. Vinjamur domain of rocks is exposed in mainly eastern part of the study area. Metabasalt/amphibolite is exposed in the low lying area, lit par lit injection migmatite occurring as patches within metabasalt and quartzite is forming linear N-S trending ridges, intrusive granite occurring as isolated hill and also exposed in low lying areas. Udayagiri domain mainly comprises of phyllite, garnet biotite schist, chloritoid-garnet schist and quartzite and younger intrusive granite. Maximum part of the study area is covered by phyllite. The garnet biotite schist, chloritoid garnet schist is present as narrow linear N-S trending patches and quartzite are occurring as N-S trending linear ridge. The highest grade of metamorphism in the Udayagiri domain is upper greenschist facies and in Vinjamuru domain is upper amphibolites facies. At the contact between the two domains the S_1 foliation/schistosity

of both the metabasalt and the metapelitic trends NNW-SSE and show steep to moderate dip towards west/southwest (Fig. 1a). Near the contact between the two groups, in chloritoid-garnet schist (Fig. 1a) of Udayagiri domain (consisting mainly of quartz, muscovite, paragonite, Spessartine garnet, chlorite, chloritoid and magnetite as accessory mineral), four small grains of xenotime have been identified by EPMA study among which three have been used for age determination.

In the chloritoid-garnet schist two types of garnets are found. One is pre-tectonic to S_1 schistosity (Fig. 4b) and the other is syn-tectonic with the S_1 schistosity, formed during D_1 phase of deformation (Fig. 4a). Both the garnets show alteration to chlorite in their marginal parts (Fig. 4a,b); Some garnet grains are found to be completely pseudomorphed by chlorite (Fig. 4c). Along with xenotime, grains of monazite, zircon, apatite and tourmaline have also been found within the metapelitic. Small grains of thorite and monazite are also present within the matrix. The xenotime grains have been analysed through EPMA for major oxides and REEs. Fifteen points were analysed from three grains and fifteen dates obtained using the software Age Quant of SX-Peak sight. (Table 1 and 2, Fig. 5). The youngest age obtained was 1708 Ma and the oldest, 2190 Ma (Fig. 5), average age being 1921 ± 120 ma (MSWD=0.43).

Analytical Condition

The analysis was carried out on CAMECA SX 100 with 5 wavelength spectrometers at GSI, Hyderabad. The analytical conditions included accelerating voltage of 20 KV and beam current of 100 nA with a beam diameter of 1 μm. The standards used for the analysis of major oxides were natural silicates and glass for REE. The X-ray lines selected were Si K α (Orthoclase), PK α (apatite), La L α (La glass), Ce L α (Ce glass), Pr L α (Pr glass), Nd L α (Nd glass), Sm L α (Sm glass), Eu L α (Eu glass), Gd L α (Gd glass), Tb L α (Tb glass), Dy L α (Dy glass), Ho L α (Hoglass), Er L α (Er glass), Tm L α (Tm glass), Yb L α (Yb glass), Lu L α (Lu glass), Y L α (YAG), Zr L α (Zircon), Ca K α (Wollaastonite), Fe K α (Almandine), Pb M α (Pyromorphite), Th M α (Th glass), U M α (U glass). An empirical correction for element interferences PbM α –ThM α , PbM α –YL α and UM α –ThM α N α were applied before the calculation of ages.

Use of Xenotime for Geochronology

Xenotime is a rare earth phosphate mineral with the formula yttrium orthophosphate (YPO_4). Xenotime crystallizes in tetragonal system (Rasmussen 2005) and consists of PO_4 tetrahedra separated by REO_8 octahedra (Yunxiang et. al. 1995) and preferentially incorporates

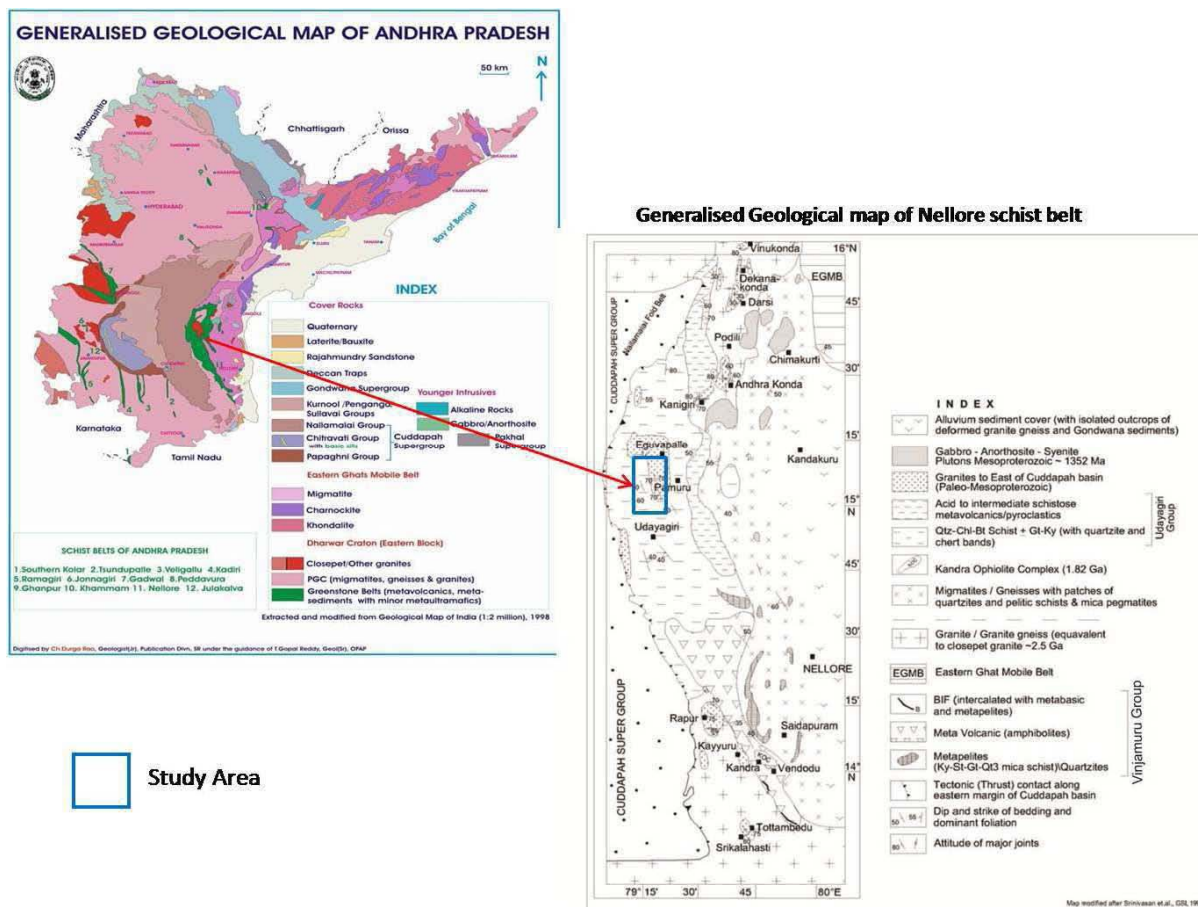


Fig.1. Generalized geological map of the NSB.

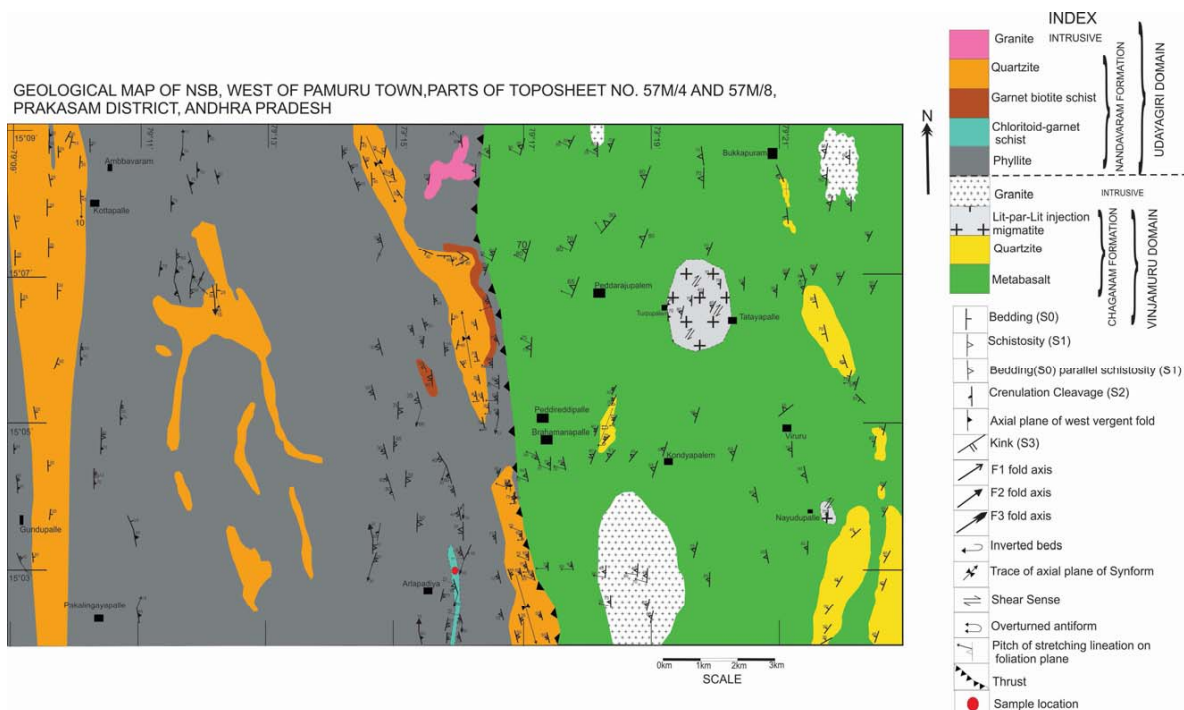


Fig.1a. Geological map of the study area.

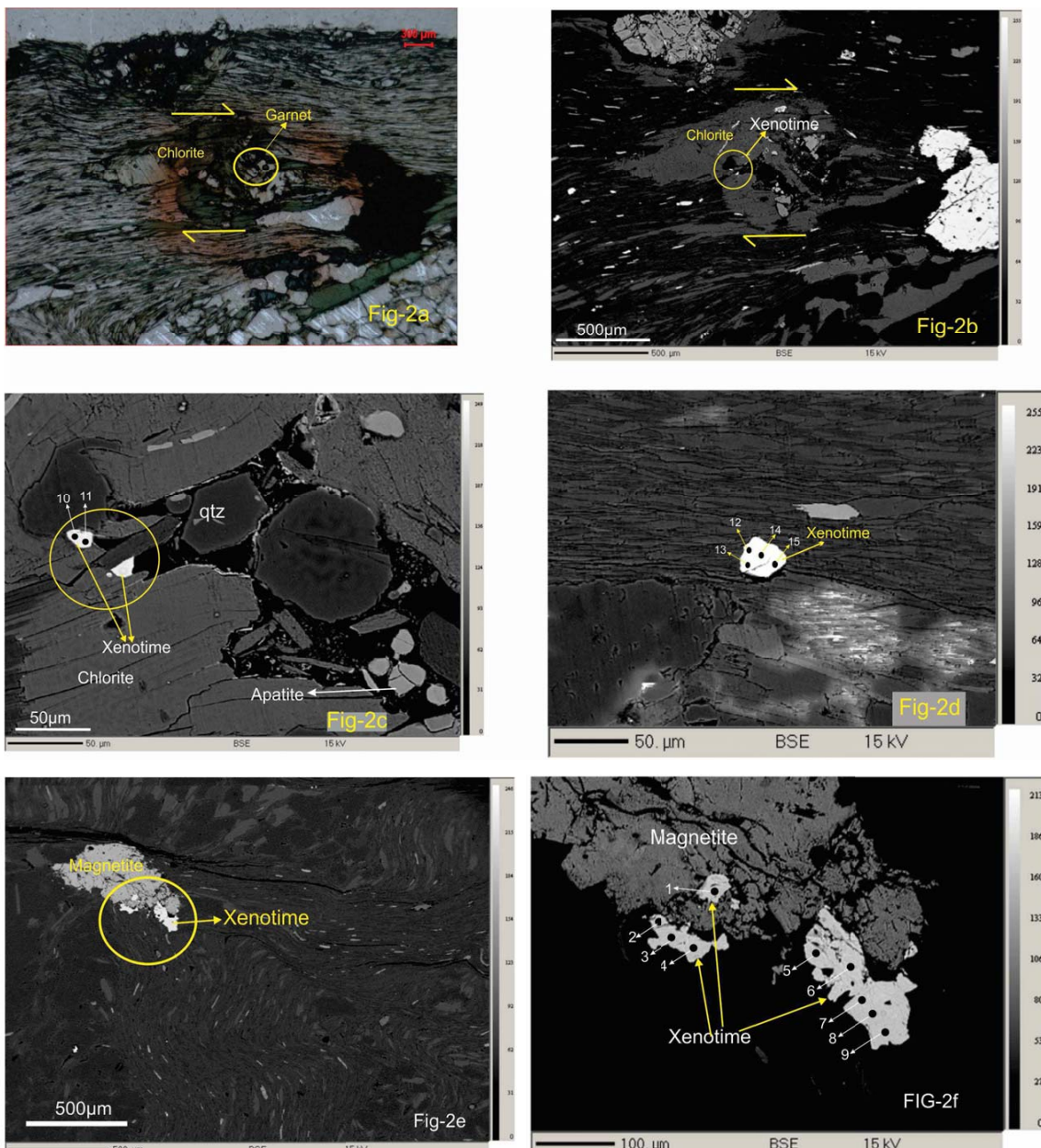


Fig.2. (a) Photomicrograph of syntectonic popyroblast of Chlorite (PPL) with preserved core of garnet. (b) BSE image of (2a), showing xenotime grains(Grain-1). (c) Zoomed BSE image of (2b), Black circles numbered 10, 11 indicate EPMA analysis points. (d) BSE image of xenotime grain (grain-2) occurring within the matrix. Black circles numbered 12,13,14,15 indicate EPMA analysis points. (e) BSE image of Xenotime grains (grain-3) occurring with magnetite grain. (f) Zoomed view of (2e). Black circles indicate EPMA analysis points.

smaller HREEs and yttrium. The mineral is isostructural with zircon. It is a common accessory mineral in granites and pegmatites, a common detrital mineral in siliciclastic sedimentary rocks and also occurs in pelites and medium to high grade metamorphic rocks. Zircon is the most used U-Pb chronometer. Monazite is also used as a U-Pb chronometer and is preferred over xenotime as the former is commonly more abundant and larger in size. Xenotime

can be especially helpful for dating diagenetic age of sedimentary rocks. Several dating techniques are used to date xenotime such as SIMS, SHRIMP (Rasmussen et al. 2004; Rasmussen, 2005) and EPMA (Suzuki et al. 1991; Asami et.al. 2002). Xenotime has high U content and very low initial Pb concentration, so it is ideal for U-Pb geochronology (Cherniak, 2006). There are two possible mechanism by which U and Th are concentrated in xenotime

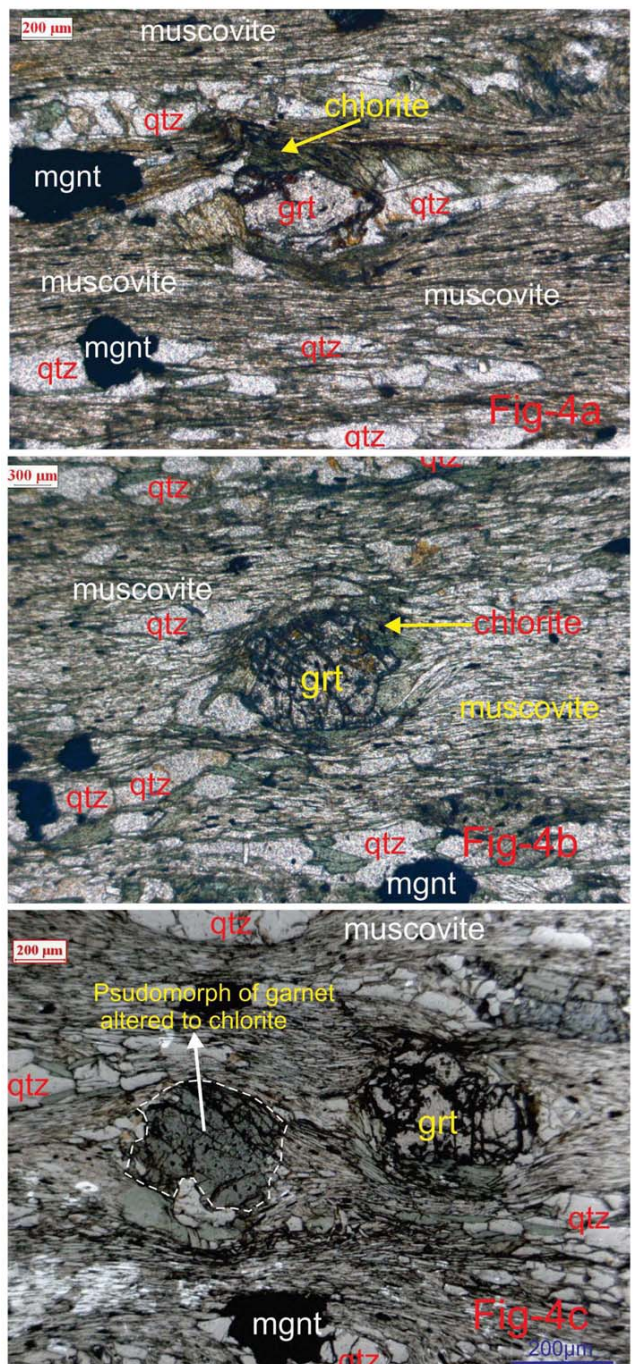
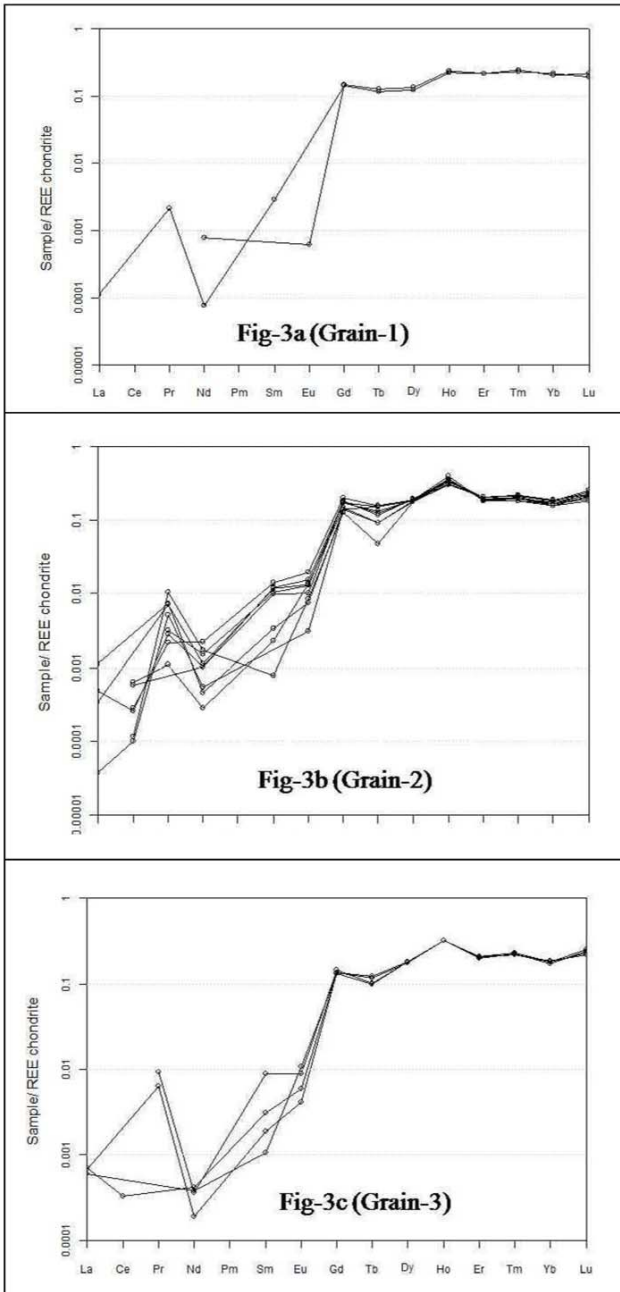


Fig.3. Chondrite normalized REE diagram of (a) 2 analyses from grain -1. (b) 9 analyses from grain-2 and (c) 4 analyses from grain -3 (normalising values after Nakamura, 1974).

structure, substitution 1: $(\text{REE}, \text{Y})^{3+} + \text{P}^{5+} = (\text{Th}, \text{U})^{4+} + \text{Si}^{4+}$, substitution 2 : 2 $(\text{REE}, \text{Y})^{3+} = (\text{U}, \text{Th})^{4+} + \text{Ca}^{2+}$. Pb diffusion is very slow in xenotime compared to REE diffusion (Cherniak 2006). In zircon Pb diffusion occurs at the same rate or faster than REEs. In monazite also Pb diffusion is faster than in xenotime (Cherniak, 2006). Closure temperatute of Pb is also very high in xenotime, A grain with an effective radius of 10 microns will have a closure temperature around 890°C and a 50 micron grain is

Fig.4. PPL image of alteration of (a) syn-tectonic garnet to chlorite at its marginal part. (b) alteration of pre-tectonic garnet to chlorite at its marginal part. (c) of Psuedomorph of pre-tectonic garnet fully altered to chlorite. The boundary of psuedomorph of garnet is marked by white dashed line. Qtz=quartz, mgnt=magnetite.

characterized by a closure temperature of 980°C (Cherniak, 2006). Hence xenotime is very resistant to Pb loss due to later hydrothermal alteration. The above characters make xenotime a robust U-Pb chronometer.

Table 1. EPMA Analysis of xenotime

DataSet/ Point	1 / 1 .	2 / 1 .	3 / 1 .	4 / 1 .	5 / 1	6 / 1 .	7 / 1	8 / 1 .	9 / 1 .	10 / 1 .	11 / 1 .	12 / 1	13 / 1	14 / 1 .	15 / 1 .
	Grain-2	Grain-1	Grain-1	Grain-3	Grain-3	Grain-3	Grain-3								
SiO ₂	0.27	0.305	0.201	0.307	0.447	0.169	0.229	0.043	0.083	0.017	0.152	0.026	0.046	0.118	0.157
P ₂ O ₅	35.254	35.396	34.381	34.109	34.44	34.383	34.85	35.529	34.796	36.191	35.078	34.941	35.206	35.227	35.018
CaO	0.01	0.013	0.029	0.027	0.04	0.024	0.005	-0.016	-0.004	-0.007	0.02	-0.001	-0.004	0.006	-0.01
Y ₂ O ₃	42.766	41.005	41.822	41.003	41.24	41.18	41.53	42.743	41.95	42.339	41.937	42.183	42.686	42.63	42.63
La ₂ O ₃	-0.013	0.03	0.009	0.013	-0.014	-0.004	-0.01	-0.096	0.001	0.003	-0.02	0.019	0.018	-0.028	0.016
Ce ₂ O ₃	0.045	-0.001	-0.026	0.018	-0.008	0.02	0.041	0.008	0.007	-0.001	-0.012	0.023	-0.029	-0.024	-0.006
Pr ₂ O ₃	0.01	0.068	0.066	0.026	0.029	0.02	0.054	0.09	0.029	0.02	-0.037	-0.023	0.059	0.085	-0.065
Nd ₂ O ₃	0.015	0.024	0.059	0.054	0.08	0.116	0.207	0.013	-0.02	0.004	0.041	0.022	0.01	0.019	0.02
SmO	0.039	0.057	0.2	0.167	0.177	0.239	-0.02	0.096	0.047	0.049	-0.003	0.053	0.032	0.149	0.018
PbO	0.312	0.301	0.35	0.397	0.448	0.334	0.379	0.24	0.259	0.112	0.127	0.217	0.202	0.206	0.199
UO ₂	0.851	0.894	1.03	1.251	1.334	0.809	1.088	0.642	0.711	0.357	0.424	0.512	0.481	0.514	0.529
ThO ₂	0.408	0.407	0.576	0.731	0.775	0.521	0.576	0.29	0.313	0.018	0.026	0.248	0.233	0.246	0.259
ZrO ₂	0	0	0	0	0	0	0	0	0	0	0	0	0	0	0
Yb ₂ O ₃	3.896	3.984	3.636	3.659	3.64	3.466	3.425	4.015	4.054	4.465	4.811	3.728	3.894	3.862	3.96
Dy ₂ O ₃	5.836	5.943	6.09	6.229	6.061	5.946	6.03	5.687	5.725	4.002	4.327	5.578	5.705	5.744	5.777
Ho ₂ O ₃	2.087	2.244	2.285	2.328	2.407	2.61	2.332	2.171	1.992	1.497	1.578	2.087	2.115	2.106	2.101
Er ₂ O ₃	4.472	4.39	4.134	4.092	4.072	3.913	4.091	4.451	4.433	4.716	4.694	4.26	4.436	4.436	4.311
Tm ₂ O ₃	0.558	0.614	0.537	0.568	0.59	0.537	0.578	0.638	0.635	0.717	0.664	0.642	0.66	0.633	0.631
FeO	-0.059	-0.04	0.16	0.181	0.125	0.343	0.008	0.025	0.016	1.21	1.228	-0.063	-0.085	-0.08	-0.103
EuO	0.088	0.049	0.087	0.066	0.084	0.127	0.101	0.055	0.02	-0.008	0.004	0.038	0.027	0.057	0.07
Lu ₂ O ₃	0.744	0.822	0.771	0.65	0.703	0.616	0.722	0.855	0.769	0.744	0.665	0.804	0.851	0.764	0.732
Gd ₂ O ₃	3.67	3.477	4.32	4.595	4.339	5.044	4.431	3.241	3.47	3.56	3.67	3.391	3.359	3.607	3.269
Tb ₂ O ₃	0.401	0.66	0.561	0.501	0.664	0.677	0.531	0.208	0.396	0.503	0.556	0.507	0.527	0.432	0.42
Total	101.66	100.64	101.28	100.970	101.7	101.09	101.2	100.16	99.682	100.51	99.93	99.193	100.43	100.71	99.933
Age (Ma)	1957	1837	1813	1708	1791	2089	1863	2000	1961	1885	1811	2190	2182	2104	1999
Age err(Ma)	218	208	201	189	194	226	232	338	226	261	217	254	258	249	240

Table 2. Recalculation of xenotime analysis on the basis of four oxygen

DataSet/ Point	1 / 1 .	2 / 1 .	3 / 1 .	4 / 1 .	5 / 1	6 / 1 .	7 / 1	8 / 1 .	9 / 1 .	10 / 1 .	11 / 1 .	12 / 1	13 / 1	14 / 1 .	15 / 1 .
	Grain-2	Grain-1	Grain-1	Grain-3	Grain-3	Grain-3	Grain-3								
Si	0.009	0.0101	0.0067	0.0102	0.015	0.0056	0.008	0.0014	0.0028	0.0006	0.0051	0.0009	0.0015	0.00392	0.00522
P	0.9923	0.9963	0.9678	0.9601	0.969	0.9678	0.981	1.0001	0.9794	1.0187	0.9874	0.9835	0.991	0.99157	0.985685
Ca	0.0004	0.0005	0.001	0.001	0.001	0.0009	2E-04	-6E-04	-1E-04	-2E-04	0.0007	-4E-05	-1E-04	0.00021	-0.00036
Y	0.7604	0.7615	0.7436	0.7290	0.733	0.7322	0.738	0.76	0.7459	0.7528	0.7457	0.75	0.759	0.75799	0.757988
La	-0.0002	0.0004	0.0001	0.0002	-2E-04	-5E-05	-0	-0.001	1E-05	4E-05	-2E-04	0.0002	0.0002	-0.0003	0.000197
Ce	0.0006	-1E-05	-3E-04	0.0002	-1E-04	0.0002	5E-04	1E-04	9E-05	-1E-05	-1E-04	0.0003	-4E-04	-0.0003	-7.3E-05
Pr	0.0001	0.0008	0.0008	0.0003	4E-04	0.0002	-0	0.0012	0.0006	0.0002	-5E-04	-0.0003	0.0007	0.00103	-0.00079
Nd	0.0002	0.0003	0.0007	0.0006	1E-03	0.0014	6E-04	0.0011	0.0003	5E-05	0.0005	0.0003	0.0001	0.00023	0.000239
Sm	0.0005	0.0007	0.0024	0.002	0.002	0.0029	0.002	0.0002	-2E-04	0.0006	-4E-05	0.0006	0.0004	0.00179	0.000216
Pb	0.0028	0.0027	0.0031	0.0036	0.004	0.003	0.003	0.0021	0.0023	0.001	0.0011	0.0019	0.0018	0.00184	0.001781
U	0.0063	0.0066	0.0076	0.0093	0.01	0.006	0.008	0.0047	0.0053	0.0026	0.0031	0.0038	0.0036	0.0038	0.003913
Th	0.0031	0.0031	0.0044	0.0055	0.006	0.0039	0.004	0.0022	0.0024	0.0001	0.0002	0.0019	0.0018	0.00186	0.00196
Zr	0	0	0	0	0	0	0	0	0	0	0	0	0	0	0
Yb	0.0397	0.0406	0.037	0.0373	0.037	0.0353	0.035	0.0409	0.0413	0.0455	0.049	0.038	0.0397	0.03935	0.040349
Dy	0.0628	0.064	0.0656	0.0671	0.065	0.064	0.065	0.0612	0.0616	0.0431	0.0466	0.0601	0.0614	0.06184	0.062193
Ho	0.0222	0.0238	0.0243	0.0247	0.026	0.0277	0.025	0.0231	0.0212	0.0159	0.0168	0.0222	0.0225	0.02238	0.022328
Er	0.0469	0.0461	0.0434	0.043	0.043	0.0411	0.043	0.0467	0.0465	0.0495	0.0493	0.0447	0.0466	0.04657	0.045256
Tm	0.0058	0.0064	0.0056	0.0059	0.006	0.0056	0.006	0.0066	0.0066	0.0075	0.0069	0.0067	0.0069	0.00659	0.006567
Fe	-0.0016	-0.0011	0.0044	0.005	0.003	0.0095	2E-04	0.0007	0.0004	0.0336	0.0341	-0.0018	-0.002	-0.0022	-0.00286
Eu	0.001	0.0006	0.001	0.0008	1E-03	0.0015	0.001	0.0007	0.0002	-1E-04	5E-05	0.0005	0.0003	0.00068	0.000833
Lu	0.0075	0.0083	0.0078	0.0066	0.007	0.0062	0.007	0.0086	0.0078	0.0075	0.0067	0.0081	0.0086	0.00771	0.007387
Gd	0.0407	0.0385	0.0479	0.0509	0.048	0.0559	0.049	0.0359	0.0384	0.0394	0.0407	0.0376	0.0372	0.03996	0.036212
Tb	0.0044	0.0072	0.0062	0.0055	0.007	0.0074	0.006	0.0023	0.0043	0.0055	0.0061	0.0056	0.0058	0.00474	0.00461
Total	2.0048	1.9850	1.9811	1.9810	1.986	1.9784	1.983	1.9981	1.9672	2.024	1.9991	1.9647	1.9861	1.9912	1.978847

Table 3. EMPA analysis of garnet

DataSet/Point	Na ₂ O	Al ₂ O ₃	SiO ₂	P ₂ O ₅	CaO	TiO ₂	MnO	FeO	K ₂ O	Cr ₂ O ₃	MgO	ZnO	Y ₂ O ₃	Ce ₂ O ₃	Total
1 / 1 .	0.016	20.074	37.82	-0.07	2.581	0.114	13.143	23.73	0.009	0.009	1.244	0.061	-0.028	0.059	98.762
2 / 1 .	-0.01	21.78	37.01	-0.01	2.591	0.029	12.969	23.791	0	0.049	1.293	0.054	0.042	-0.105	99.48

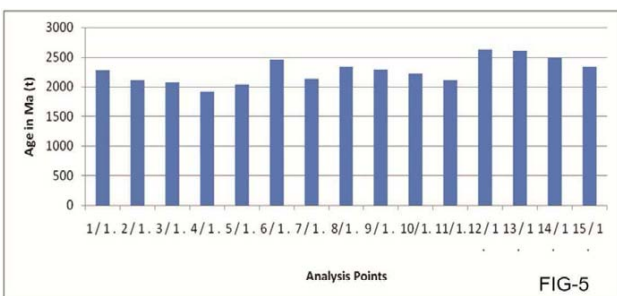


FIG-5

Fig.5. Bar diagram showing plots of apparent ages with respect to individual analysis points

Effect of Metamorphism on Xenotime

Diagenetic xenotime is stable under lower green schist facies condition but is replaced by garnet in mid to upper green schist facies condition (Rasmussen, 2005). Detrital xenotimes are stable under mid- to upper-greenschist facies condition but are very rare in amphibolites facies conditions (Rasmussen, 2005; Rasmussen et al. 2011). The Y which is released during the breakdown of detrital and diagenetic xenotime during metamorphism is preferentially incorporated into garnet structure as garnet is the repository for HREEs. In amphibolites facies condition breakdown of garnet into staurolite will release the HREEs which may then be incorporated into xenotime structure (Rasmussen, 2005).

General Geochemical and Textural Properties of Xenotime of Different Origin

Detrital, diagenetic and hydrothermal xenotimes can be differentiated on the basis of textural and geochemical criteria. Detrital xenotimes are mainly of larger size (20–200 micron) and are rounded to sub-rounded in morphology, extensively pitted and generally contain inclusions of uranium and thorium. Diagenetic xenotime mostly occurs as small pyramidal outgrowths on zircon grains. In a chondrite normalised REE diagram diagenetic xenotime shows negligible Eu anomaly and relative enrichment in MREEs especially Gd, Dy and Tb compared to HREE (Kositcin et al. 2003). In a chondrite normalised diagram igneous xenotime shows a relatively smooth HREE pattern and a characteristic negative Eu anomaly (Kositcin et al. 2003).

Hydrothermal xenotimes are strongly zoned and occur as overgrowths on detrital zircon grains and as vein and fracture fills within zircon grains (Kositcin et al. 2003). In a chondrite normalised REE diagram these show negligible Eu anomaly and enrichment of MREE over HREE compared to detrital and diagenetic xenotimes (Kositcin et al. 2003). Metamorphic xenotime tends to grow over a small core of

detrital xenotime and generally tends to get aligned with the main deformational fabric (Rasmussen et al. 2011). There is a strong compositional difference between the igneous core and metamorphic rim and the interface is marked by inclusions of quartz, and minerals rich in U and Th (Rasmussen et al. 2011).

Textural and Geochemical Characteristics of Xenotime from the Present Study

Three xenotime grains were selected for EPMA analysis during the present study. Of the three one was found included within a syntectonic porphyroblast of chlorite (grain-1) showing dextral sense of shearing. This chlorite grain is formed by retrogradation of a garnet grain, as garnet is preserved at the core of the chlorite grain (Fig.2a,b). The second (grain-2) large grain (nearly 100 microns) was found associated with a large grain of magnetite (Fig.2e,f), and the third grain (grain-3) was found to be associated with quartz, chlorite and muscovite (Fig.2d). None of the grains analysed appear to show diagenetic characters as they do not form overgrowths around zircon crystals. The grains also do not show inclusions of uranium and thorium at the centre. Presence of U, Th in the core of the xenotime will be reflected in BSE image, as U, Th will appear as more bright specs and will give a whiter tone than xenotime (Koscitsin et al. 2003) which generally found in detrital xenotime. None of the grains show core and rim structure in the BSE photographs as the igneous core will be bounded by smalls bright specs of U, Th and quartz (Rasmussen et al. 2011). Such evidences are not present in BSE images of any of the xenotime grains.

Of the 15 points analysed, Y_2O_3 is the most abundant oxide ranging from 41.18–42.825 wt%. Other ranges include Dy_2O_3 from 4.002 to 6.229 wt%, Yb_2O_3 from 3.425 to 4.811 wt%, Gd_2O_3 from 3.241 to 5.004 wt%, Tb_2O_3 from 0.208 to 0.677 wt%, Er_2O_3 from 3.913 to 4.716 wt%, Ho_2O_3 from 1.497 to 2.61 wt%, Tm_2O_3 from 0.208 to 0.677 wt% and Lu_2O_3 from 0.616 to 0.855 wt%. In chondrite normalized REE diagram all the grains show same pattern. All the 15 points taken from the three grains show a pronounced positive anomaly of Pr and a pronounced negative anomaly of Nd, a slight negative anomaly of Eu and Tb and a slight positive anomaly of Ho (Fig.3a,b,c). Plots of analysis of individual grains in chondrite normalized REE diagram (Fig.3a,b,c) shows similar character for all the grains, which suggest that they may have had similar origin. It has also been observed that there is direct correlation between the UO_2 and ThO_2 content of the xenotime grains and their age, higher the value of UO_2 and ThO_2 younger is the age and vice versa (Fig.7a,b). In grain-3, the analysed points

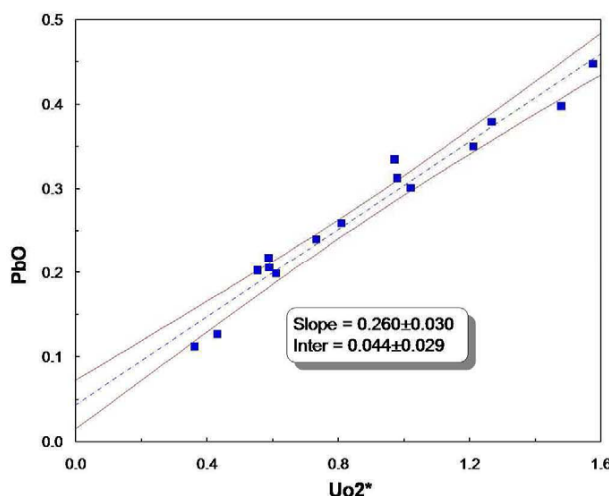


Fig.6. Plot of PbO vs UO₂*

12,13,14,15 show variation in UO₂ and ThO₂ (Fig.7b). The age of the analysed points are also varying beginning from 2200Ma and ending at 2000Ma. That means the grain started crystallizing at 2200Ma and continued up to 2000 Ma.

Chime Age Calculation of Xenotime: The Chime age calculation programme was first introduced by Suzuki et. al. (1991a, 1991b). In the Chime age calculation, an apparent age (*t*) is obtained by PbO, ThO₂ and UO₂ contents available from the EPMA, by subsequently solving the equation:

$$\text{PbO/Wpb} = \text{ThO}_2/\text{Wth}\{\exp(\lambda_1 t)-1\} + \text{UO}_2/\text{Wu}[\{\exp(\lambda_2 t+137.88)\exp(\lambda_3 t)\}/138.88-1] \quad (\text{a})$$

W is molecular weight of each oxide. Wpb is 224 for monazite and 222 for xenotime and zircon. Wth=264, Wu=270, ²³⁸U/²³⁵U=138 and λ is the decay constant for each isotope. $\lambda_{232}=4.9475*10^{-11}/\text{y}$, $\lambda_{235}=9.8485*10^{-11}/\text{y}$, $\lambda_{238}=1.55125*10^{-10}/\text{y}$ (Steiger and Jager,1977). The apparent age is used to determine the sum of ThO₂ and UO₂ as ThO₂* (monazite), and UO₂*(zircon and xenotime) by the equation

$$\text{ThO}_2^* = \text{ThO}_2 + \text{UO}_2^* \text{Wth}/\text{Wu}\{\exp(\lambda_{232})-1\} * [\{\exp(\lambda_{235}t)+138\exp(\lambda_{238}t)\}]/138-1 \quad (\text{b})$$

$$\text{UO}_2^* = \text{UO}_2 + 139.\text{ThO}_2.\text{Wu}\{\exp(\lambda_{232}t)-1\} / \text{Wth.}\{\exp(\lambda_{235}t)+138\exp(\lambda_{238}t)-139\} \quad (\text{c})$$

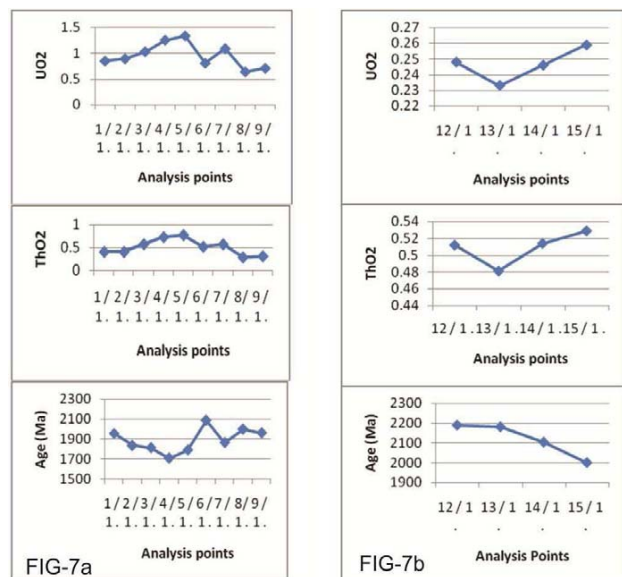


Fig.7. Corelation between UO₂ and ThO₂ content of the grain and the age of (a) grain-2, associated with magnetite. (b) grain-3, occurring as isolated grain within the matrix.

The plot of UO₂* and ThO₂* vs PbO will lie on a straight line if the grains are monogenetic and remained in closed system. The relation between PbO, ThO₂* and UO₂* is given by

$$\text{PbO} = m \text{ThO}_2^* + b \text{ (monazite)} \quad (m \text{ is slope and } b \text{ is the intercept of the straight line})$$

$$\text{PbO} = m \text{UO}_2^* + b \text{ (zircon and xenotime)}$$

The intercept *b* determines the amount of initial Pb present. If the straight line passes through the origin then the amount of initial lead is zero. Deviation of the straight line from the origin represents presence of initial lead or lead loss by some process. The slope value *m* is used for determining the first approximation age *T*. The apparent age *t* is substituted by the first approximation age *T* to determine second approximation age.

$$T = 1/\lambda_{232} \ln(1+m \text{Wth}/\text{Wpb}) \text{ (monazite)} \quad (\text{d})$$

$$m.(\text{Wu}/\text{Wpb}) = [\{\exp(\lambda_{235}T) + 138\exp(\lambda_{238}T)\}/138]-1 \text{ (xenotime and zircon)} \quad (\text{e})$$

CHIME age of xenotime, present study: The apparent ages (*t*) for fifteen points of the three grains are obtained by solving equation-a are given below (all ages are in Ma)

1 / 1	2 / 1	3 / 1	4 / 1	5 / 1	6 / 1	7 / 1.	8 / 1.	9 / 1	10 / 1.	11 / 1.	12 / 1	13 / 1	14 / 1	15 / 1
Grain-2	Grain-1	Grain-1	Grain-3	Grain-3	Grain-3	Grain-3								
2279	2107	2066	1917	2030	2454	2135	2341	2289	2212	2105	2631	2607	2491	2331

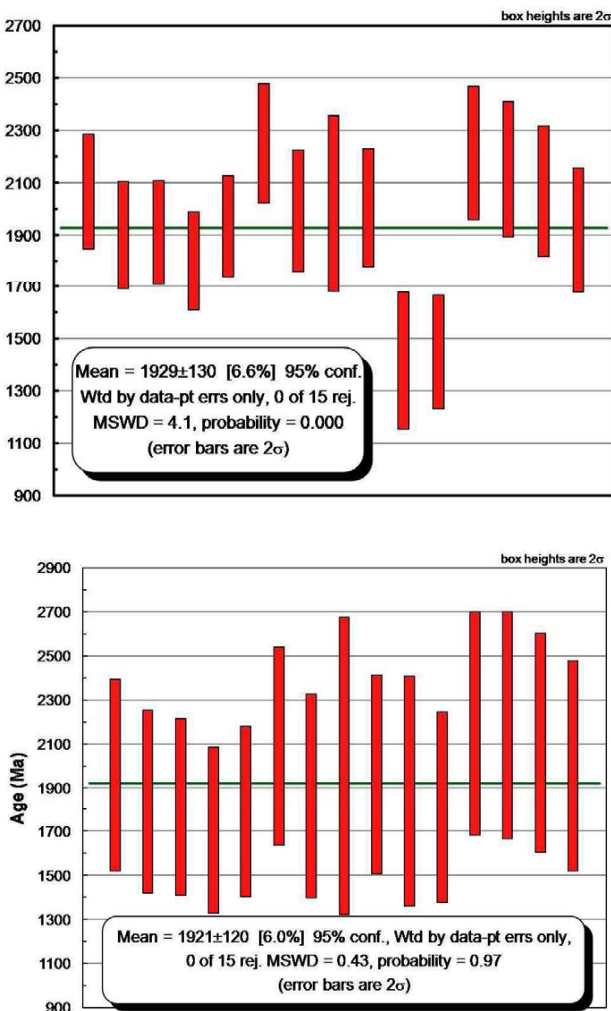


Fig.8. (a) Point age dispersion for CHIME age in relation to the weighted averages (smooth thick trace). (b) Point age dispersion for age calculated by ‘Age Quant of SX-Peak sight software’ in relation to the weighted averages (smooth thick trace).

The apparent ages are used to calculate the UO_2^* values for all the fifteen grains which are then plotted against PbO . All the points plot in a straight line with a slope (m) = 0.260 ± 0.030 and intercept (b) = 0.044 ± 0.029 (Fig.6). Then from the equation-e, the average first approximation age (T) obtained is 1929 ± 130 Ma, $\text{MSWD} = 4.1$ (Fig.8a) and the median age obtained is $1993 \pm 75/-94$ Ma. Then the apparent ages are replaced by first approximation age to get the second and third approximation ages which are 1929 ± 130 Ma. Fifteen dates from three grains have also been calculated using the software Age Quant of SX-Peak sight. The youngest age obtained is 1708 Ma and the oldest age obtained is 2190 Ma (Table 1). The average age is 1921 ± 120 Ma, $\text{MSWD} = 0.43$ (Fig.8b).

DISCUSSION AND CONCLUSION

As previously discussed, both types of garnets (pre-tectonic and syntectonic) show alteration to chlorite in their marginal parts (Fig.4a, b). At some places the whole garnet grain is found to be altered to chlorite forming pseudomorph of garnet (Fig.4c). These altered (at marginal parts) garnets do not contain much of Yttrium (Table 3); this may be due to the fact that alteration of garnets into chlorite has released the Yttrium present in the garnet structure, resulting in association of xenotime grains with the chlorite grain having preserved core of garnet. (Fig.2a,b);. Xenotime may be very rare in matrix of mid garnet zone rocks, although it may be present as inclusion within garnet and alteration of yttrium rich garnet during retrogression may also release sufficient Y to stabilize xenotime during retrogression (Spear et al. 2002). The rock in the present case occurs in mid garnet zone. But the garnets are deficient in Y. We got one xenotime occurring as isolated grain (grain-3) in the matrix. Evidence of retrogression of garnet are also present in the rock. Even one retrogressed garnet grain (Fig.2a,b) contains xenotime (grain-1) at the marginal part. So the xenotime grains in the present case may have formed due to release of Y from the garnet structure during retrogression. Hence the formation of xenotime has a strong relation with the retrogression of garnet. Thus the released Y from the garnet structure during retrogression has formed xenotime which occurs as fracture filling inside a magnetite grain as well as around the grain boundary of the same magnetite grain (Fig.2e,f). The peak temperature of metamorphism of this metapelite (chloritoid-garnet schist) is likely to be around 450°C as spessartine garnet and chloritoid are present (Rasmussen et al. 2011). Detrital xenotime has been reported to persist up to lower amphibolite facies in a chloritoid-garnet bearing quartzite of Mount Barren Group of Western Australia (Rasmussen 2005). But in the present case lack of pronounced negative anomaly of Eu in chondrite normalized REE diagram of xenotime grains precludes it being of detrital origin. This xenotime is unlikely to have formed during prograde metamorphism, in that case it would have formed around some mineral phase which contains Y such as a core of already existing detrital xenotime (Rasmussen 2005) or as inclusion within staurolite due to breakdown of garnet. Such evidences are absent in present study. Thus dating of these xenotime grains gives the age of retrograde metamorphism of the chloritoid-garnet schist of Udayagiri domain. One of the xenotime grains is associated with a retrogressed syntectonic garnet which represents D_1 phase deformation. So the retrogression of the chloritoid-garnet schist of Udayagiri domain has occurred at least after D_1 deformation. The

average calculated age of these xenotime grains is 1929 ± 130 Ma. Thus the upper age limit of the Udayagiri domain may be constrained at 1929 ± 130 ma.

Acknowledgement: The authors thank the Director General of Geological Survey of India for permitting to

publish the paper. They express their deep sense of gratitude Shri S. Balakrishnan, Deputy Director General, Southern Region, and Shri M.S. Jairam, Deputy Director General, State Unit: Andhra Pradesh for their co-operation and constant encouragement without which this investigation would not have been possible.

References

- ASAMI, M., SUZUKI, K. and GREW, E.S. (2002) Chemical Th–U–total Pb dating by electron microprobe analysis of monazite, xenotime and zircon from the Archean Napier Complex, East Antarctica: evidence for ultra-high-temperature metamorphism at 2400 Ma. *Precambrian Res.*, v.114, pp.249–275.
- CHERNIAK, D.J. (2006) Pb and rare earth element diffusion in xenotime, *Lithos*, v.88, pp.1-14.
- DHARMA RAO, C.V. and REDDY, U.V.B. (2009) Petrological and geochemical characterization of ophiolitic mélange, Nellore Khammam schist belt, SE India. *Jour. Asian Earth Sci.*, v.65, pp.261-276.
- HARI PRASAD, B., OKUDAIRA, T., DIVI, R.S. and MASARU, Y. (1999) Structural Features of the Archean Nellore–Khammam Schist Belt, Southeast India. *Jour. Geosci.*, v.42, pp.227-235.
- KOSITCIN, N., MCNAUGHTON, N.J., GRIFFIN, B.J., FLETCHER, I.R., GROVES, D.I. and RASMUSSEN, B. (2003) Textural and geochemical discrimination between xenotime of different origin in the Archean Witwatersrand Basin, South Africa. *Geochim. Cosmochim. Acta*, v.67, pp.709-731.
- MOEEN, S. (1998) P-T estimates from the Nellore schist belt (India) and evidence for the superimposed metamorphic events. *Geol. Jour.*, v.33, pp.1-15.
- NARAYANA RAO, M. (1983) Lithostratigraphy of the Precambrian rocks of the Nellore Schist Belt. *Quart. Jour. Geol. Min. Metall. Soc. India*, v.55, pp.83-89.
- NI YUNXIANG, HUGHES M. JOHN and MARIANO N. Anthony (1995) Crystal chemistry of monazite and xenotime structures, *American Mineral.*, v.80, pp.21-26.
- OKUDAIRA T., HAMAMOTO T., HARI PRASAD B. and RAJNEESH KUMAR (2001) Sm–Nd and Rb–Sr dating of amphibolite from the Nellore–Khammam schist belt, SE India: constraints on the collision of the Eastern Ghats terrane and Dharwar–Bastar craton. *Geol. Mag.*, v.138(4), pp.495–498.
- PRSEK JAROSLAV, BACIK PETER, ONDREZKA MARTIN, BUDZYN BARTOSZ and UHER PAVEL (2010) Metamorphic-hydrothermal ree minerals in the bacúch magnetite deposit, western carpathians, slovakia: (sr,s)-rich monazite-(ce) and nd-dominant hingganite. *Canadian Mineral.*, v.88, pp.81-94.
- RAMAM, P.K. and MURTY, V.N. (1997) Geology of Andhra Pradesh.
- Geological Society of India, Bangalore, 245p.
- RASMUSSEN BIRGER (2005) Radiometric dating of sedimentary rocks: the application of diagenetic xenotime geochronology, *Earth Science Rev.*, v.68, pp.197-243.
- RASMUSSEN et al. (2011) Response of xenotime to prograde metamorphism. *Contrib. Mineral. Petrol.*, v.162, pp.1259-1277.
- RASMUSSEN, B., FLETCHER, I.R., BENGTON, S. and MCNAUGHTON, N.J. (2004) SHRIMP U–Pb dating of diagenetic xenotime in the Stirling Range Formation, Western Australia: 1.8 billion-year minimum age for the Stirling biota. *Precambrian Res.*, v.133, pp.133-339.
- RAVIKANT, V. (2010) Palaeoproterozoic (1.9 Ga) extension and breakup along the eastern margin of the Eastern Dharwar Craton, SE India: New Sm–Nd isochron age constraints from anorogenic mafic magmatism in the Neoarchean Nellore greenstone belt. *Jour. Asian Earth Sci.*, v.12, pp.67-81.
- SAHA, D. (2004) Structural asymmetry and Plate tectonic set-up for a Proterozoic Fold and Thrust Belt: Nallamalai Fold Belt and Adjoining Terrane, South India. *Geol. Surv. India Spec. Publ.*, v.84, pp.101-119.
- SAHA, D., SAIN, A., NANDI, P., MAZUMDER, R. and KAR, R. (2013) Tectonostratigraphic evolution of the Nellore schist belt, southern India, since the Neoarchean, Accepted MS: Geological Society London Memoir (eds. Pat Eriksson & Rajat Mazumder) on Precambrian Basins of India: Stratigraphic and Tectonic Context.
- SPEAR, F.S. and PYLE, J.M. (2002) Apatite, monazite, and xenotime in metamorphic rocks. In: M.J. Kohn, J. Rakovan, and J.M. Hughes (Eds.), *Phosphates: Geochemical, Geobiological and Materials Importance*. *Mineral. Soc. Amer. Rev. Mineral. Geochem.*, v.48, pp.293-335.
- SUZUKI, K. and ADACHI, M. (1991) Precambrian provenance and Silurian metamorphism of the Tsubonasawa paragneiss in the South Kitakami terrane, Northeast Japan, revealed by the chemical Th–U–total Pb isochron ages of monazite, zircon and xenotime. *Geochem. Jour.*, v.25, pp.357-376.
- VASUDEVAN, D. and RAO, T.M. (1975) The high grade schistose rocks of Nellore Schist Belt, Andhra Pradesh and their geologic evolution. *Indian Mineral.*, v.16, pp.43-47.

(Received: 17 February 2014; Revised form accepted: 2 September 2014)